Molecular Crystals and Liquid Crystals

Publication details, including instructions for authors and subscription information:
http://www.tandfonline.com/loi/gmcl20

Control of the Bistable Molecular Reorientation Angle in a Nematic Liquid-Crystal-Light-Valve

S. Residori [a] & U. Bortolozzo [a]

[a] Institut Non Linéaire de Nice, Valbonne, France

Version of record first published: 22 Sep 2006

To cite this article: S. Residori & U. Bortolozzo (2006): Control of the Bistable Molecular Reorientation Angle in a Nematic Liquid-Crystal-Light-Valve, Molecular Crystals and Liquid Crystals, 454:1, 207/[609]-216/[618]

To link to this article: http://dx.doi.org/10.1080/15421400600654330

Mol. Cryst. Liq. Cryst., Vol. 454, pp. 207/[609]–216/[618], 2006

ISSN: 1542-1406 print/1563-5287 online
DOI: 10.1080/15421400600654330

Control of the Bistable Molecular Reorientation Angle in a Nematic Liquid-Crystal-Light-Valve

S. Residori
U. Bortolozzo
Institut Non Linéaire de Nice, Valbonne, France

We show experimentally that optical localized structures can be stored as elementary optical pixels lying on matrices that are impressed in a small pretilt angle of the nematics contained in a Liquid-Crystal-Light-Valve. The molecular reorientation, which is induced by an optical feedback, is bistable and may be controlled by a suitable phase profile superimposed on the input laser beam.

Keywords: liquid crystal light valves; localized structures; pattern control

INTRODUCTION

Non equilibrium processes lead in nature to the formation of spatially periodic and extended structures, so-called patterns [1]. The birth of a pattern from a homogeneous state takes place through the spontaneous breaking of one or more of the symmetries characterizing the system [2]. In some cases, the pattern is localized in a restricted region of the space, so that we deal with localized instead of extended structures. Localized structures have been recently demonstrated in several experiments based on a Liquid-Crystal-Light-Valve (LCLV) with optical feedback [3–5]. In this paper we present an experimental realization on the control of optical localized structures in a modified LCLV experiment. By inserting a spatial phase modulator (SPM) on the path of the input laser beam, we are able to store and actualize localized structures on large area matrices, that are impressed as a

U. Bortolozzo acknowledges financial support from the FUNFACS European project, n. 2005-004/004868.

Address correspondence to U. Bortolozzo, Institut Non Linéaire de Nice, UMR 6618 CNRS-UNSA, 1361 Route des Lucioles, F-06560 Valbonne-Sophia Antipolis, France. E-mail: umberto.bortolozzo@inln.cnrs.fr

pretilt angle in the nematic liquid crystal contained in the LCLV. The experimental observations are supported by a theoretical model, which is based on a physical equation derived for the liquid crystal reorientation angle under the effect of the control light. This equation is coupled with the light diffraction in the optical feedback loop. Numerical simulations of the model equations show quantitative agreement with the experimental observations and has allowed to design suitable phase profiles for the control of localized structures. Addressing of each single localized structure is achieved by local pulses sent through the SPM.

DESCRIPTION OF THE LCLV AND DERIVATION OF THE MODEL EQUATIONS

As schematically depicted in Figure 1, the LCLV is composed of a nematic liquid crystal in between a glass and a photoconductive plate over which a dielectric mirror is deposed [6]. The liquid crystals are planar aligned (nematic director $\vec{n}$ parallel to the cell walls) and the cell thickness is 15 μm. Transparent electrodes covering the glass plates permit the application of an external voltage V_0 across the liquid crystals. The photoconductor behaves like a variable impedance, its resistance decreasing when increasing the intensity of the light I_w impinging on the rear side of the LCLV (write light). Thus, the voltage V_{LC} that effectively drops across the liquid crystals is $V_{\mathrm{LC}} = \Gamma V_0 + \alpha I_w$, where V_0 is the a.c. voltage externally applied to the LCLV and Γ, α are phenomenological parameters summarizing, in the linear approximation, the response of the photoconductor (Γ is the dark transfer factor that depends on the impedances of the LCLV dielectric layers) [7].

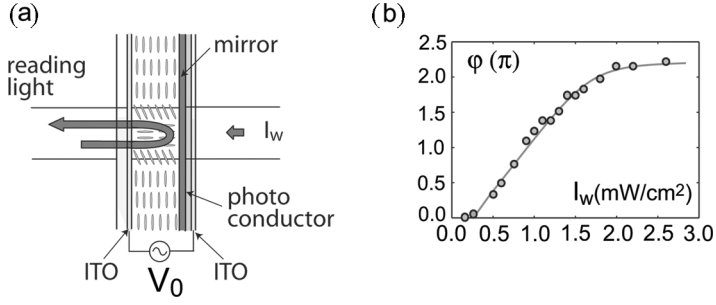

FIGURE 1 (a) Schematic representation of the LCLV and (b) its typical response as a function of the light intensity I_w, incident on the photoconductive side.

Under application of the voltage, liquid crystal molecules reorient towards the direction of the electric field [8] and, because of liquid crystal birefringence, the molecular reorientation induces a refractive index change for the light incoming on the front side of LCLV [9–11]. As a result, the input beam, which pass through the liquid crystal layer and is reflected by the mirror of the LCLV, undergoes a phase shift φ, which depends on the intensity I_w, incident on the photoconductive side and on the liquid crystal birefringence $n = n_e - n_o$, n_e and n_o being, respectively, the extraordinary (parallel to $\vec{n}$) and ordinary (perpendicular to $\vec{n}$) refractive index. For $I_w \leq 2\,\mathrm{mW/cm^2}$ the phase shift is proportional to the light intensity and the LCLV behaves like a Kerr nonlinearity. A typical response of the LCLV, showing the optical phase shift φ as a function of I_w, is shown in Figure 1b, for fixed $V_0 = 12.8\,\mathrm{V}$ and frequency $f = 6\,\mathrm{KHz}$. If θ is the average reorientation angle of the molecules, and for $\Delta n \ll n_e, n_o$ we can express the phase shift as $\varphi = \beta \cos^2\theta$, with $\beta = 2\pi\Delta n d/\lambda_0$, where λ_0 is the optical wavelength. In our experiments $\Delta n = 0.2$, with $n_e = 1.7$ and $n_o = 1.5$. Under this approximation, we can reconstruct the average tilt θ from the measured phase shift φ.

The model for the local liquid crystal reorientation angle can be derived by considering a simple approximation that neglects the dependence on the cell thickness, since the measured values of the tilt angle are integrated along z, z being the longitudinal coordinate along the cell thickness.

First, we describe the Fréedericksz transition by the usual balance between the electric and the elastic torque [8]

$$K_{11}\frac{\partial^2\theta}{\partial z^2} + \Delta\varepsilon E_{\mathrm{LC}}^2 \sin^2 2\theta = 0 \tag{1}$$

where $\Delta\varepsilon$ is the dielectric anisotropy, K_{11} the splay elastic constant and $E_{\mathrm{LC}} = V_{\mathrm{LC}}/d$ is the electric field applied across the liquid crystal. When E_{LC} exceeds the Fréedericksz transition threshold, E_{FT}, molecular reorientation takes place and the first deformation mode can be written as $\theta_M \sin(\pi z/d)$. We take the average along z, so that $\theta = \theta_M 2/\pi$.

The average reorientation angle θ is measured when $I_w = 0$, by varying the voltage V_0 and by recording the corresponding phase shift $\varphi = \beta\cos^2\theta$ on the input beam. In this conditions the electric voltage effectively applied across the liquid crystals is $V_{\mathrm{LC}} = \Gamma V_0$. The results are plotted in Figure 2 and the experimental data are fitted with the function

$$\theta = \frac{\pi}{2}\left(1 - \sqrt{\frac{V_{\mathrm{FT}}}{V_{\mathrm{LC}}}}\right),$$

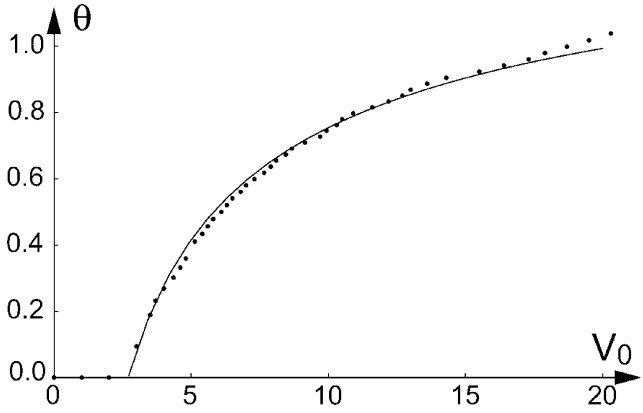

FIGURE 2 Average reorientation angle θ as a function of the voltage V_0 when the intensity I_w is zero.

with $\Gamma = 0.3$. When $I_w \neq 0$, then $V_{\mathrm{LC}} = \Gamma V_0 + \alpha I_w$, with $I_w = I_w(x,y,t)$. The round-trip time of the light circulating in the optical loop is much shorter than the typical response time of the liquid crystals, so that we consider that the light distribution instantaneously follows the θ distribution. Hence, we can write for the average director tilt, $0 < \theta < \pi/2$, a local relaxation equation, which takes into account the transverse dependence of $\theta = \theta(x,y)$, once it is coupled to the feedback write intensity I_w [12]:

$$\tau \partial_t \theta = l^2 \nabla_\perp^2 \theta - \theta + \frac{\pi}{2}\left(1 - \sqrt{\frac{V_{\mathrm{FT}}}{\Gamma V_0 + \alpha I_w(\theta)}}\right) \tag{2}$$

where $\nabla_\perp^2$ is the transverse Laplacian, l is the diffusion length, τ the local relaxation time, $\Gamma V_0 + \alpha I_w$ is the effective voltage across the liquid crystals. From the experimental characteristics of the LCLV we can evaluate $\Gamma = 0.3$, $\alpha = 2.5\,\mathrm{Vcm^2/mW}$ and $V_{\mathrm{FT}} = 1.05\,V$. The response time is proportional to the rotational viscosity of the liquid crystal and its typical value is around $\tau = 30\,\mathrm{ms}$. The diffusion length l can be estimated approximately to $40\,\mu\mathrm{m}$, and it is mainly due to the diffusion of charges in the photoconductor. Recently it has been directly measured for a photorefractive LCLV [13], however similar values have been obtained from indirect measurements performed in a semiconductor LCLV [3]. The electric coherence length l_e of the liquid crystal can be evaluated in the single constant approximation [14], $l_e = (d/\alpha I_w)\sqrt{K/\varepsilon_0 \Delta\varepsilon}$, where $\alpha I_w/d$ is the equivalent electric field due to the feedback light and K is the elastic constant of the liquid

crystals. By considering that for the planar geometry a transverse deformation is mainly a twist, by taking typical values, $K = K_{22} = 13\,\text{pN}$, $\Delta\varepsilon = 15$, $\alpha I_w = 2\,\text{V}$ and $d = 15\,\mu\text{m}$, we get $l_e \simeq 3\,\mu\text{m}$, which is fairly smaller than l.

THE OPTICAL FEEDBACK LOOP AND THE PHASE CONTROL

As shown in Figure 3, the optical feedback is obtained by sending back onto the photoconductor the light that has passed through the liquid-crystals and has been reflected by the mirror of the LCLV. Two lenses, L_1 and L_2, form an image of the front side of the LCLV on the plane marked by a dashed line. An optical fiber bundle closes the loop, transporting the image from one end to the other with negligible losses and with a spatial resolution of $20\,\mu\text{m}$. The free propagation length is $L = 80\,\text{mm}$, over which diffraction takes place. For such a diffractive feedback, the system is known to display a transverse spatial instability [3], developing hexagonal patterns at a typical wavelength $\sqrt{2\lambda L}$ [15].

In the present experiment, the beam splitter (CS) at the entrance of the optical loop is a polarizing cube, so that it transmits the vertical polarization and reflects the horizontal one. The liquid crystal director is at 45° with respect to the input polarization, which is vertical. Since the beam reflected by the cube is horizontally polarized, the feedback loop produces polarization interference between the ordinary and extraordinary waves. Then the electric field reflected by the beam splitter CS is

$$E_p = \frac{E_{\text{in}}}{2}\left(1 - e^{-i\varphi(I_w)}\right)$$

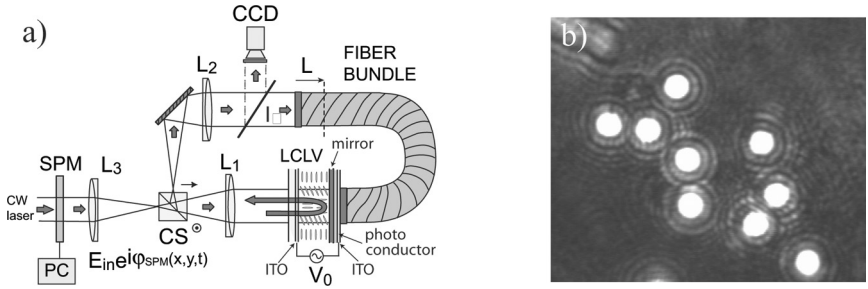

FIGURE 3 (a) Experimental setup for the LCLV with optical feedback; (b) localized structures typically observed in the near-field (CCD camera) at $I_{\text{in}} = 0.51\,\text{mW/cm}^2$.

where E_{in} is the transvers electric field produced by an enlarged and collimated He-Ne laser, wavelength $\lambda_0 = 632.8\,\text{nm}$. The intensity on the photoconductor is $I_w = |\, D_\perp \cdot E_p \,|^2$ where $D_\perp$ is the diffraction operator $D_\perp = e^{(i\lambda_0 L/4\pi)\nabla_\perp^2}$ [3].

As schematically depicted in Figure 3, the setup includes also a spatial phase modulator (SPM) connected to a personal computer (PC) and inserted in the optical path of the input beam E_{in}. The SPM is a twisted nematic liquid crystal display without polarizers [16]. The polarization of the beam impinging on the SPM is parallel to the entrance extraordinary axis, which is at 45° with respect to the vertical polarization. For such a geometry, the SPM induces on the beam incident on the LCLV a phase shift φ_{SPM} that is a function of the gray level set on the PC. We have measured φ_{SPM} varying from 0 to π when the gray level changes from 0 to 255.

Taking into account all the contributions described previously, the light intensity on the photoconductor is

$$I_w = \frac{I_{\text{in}}}{4}\left| D_\perp \cdot [e^{i\varphi_{\text{SPM}}(x,y)}(1 - e^{-i\beta\cos^2\theta})]\right|^2. \tag{3}$$

The presence of both diffraction and interference ensures multistability between differently oriented states of the liquid crystals and leads to the appearance of stable localized structures [4,5,12]. The existence of localized states in our case is due to the bistability between an homogeneous stationary solution and an hexagonal solution [3]. Numerical simulations of the model equations Eqs. (2), (3) show the appearance of localized structures in the region of bistability between two differently oriented states. The size of each localized structure is $420 \pm 30\,\mu\text{m}$ and depends on the square root of the free propagation length $\sqrt{L}$ [3]. The sinusoidal voltage applied to the LCLV is fixed to $V_0 = 12.8\,\text{V}$ and frequency $f = 6\,\text{KHz}$.

It has been numerically demonstrated for a Kerr-like system that localized structures behave like single particles moving in the presence of phase/intensity gradients [17]. In the case of LCLV and for the parameters used here, numerical simulations have shown that phase gradients are more efficient in displacing localized structures than intensity gradients are, and that localized structures go towards the maxima of the phase [18]. In the experiment, due to phase inhomogeneities, localized structures move, interact and form bound states as shown in Figure 3b. In order to avoid the crosstalk between localized structures, it has been numerically demonstrated [17] that a phase grid is able to pin localized structures on the local maxima of the grid. The physical origin of the pinning mechanism has to be searched in a

small and local reorientation of the liquid crystal director in correspondence with the local phase maxima of the input beam.

We have sent through the SPM an egg-box profile that modulates the phase of the input beam [19]. Thus, after the cube splitter, the input beam is phase modulated with a periodic two-dimensional grid $\varphi_{\mathrm{SPM}} = \varepsilon(\cos Kx + \cos Ky)^2$, where $K = 0.015\,\mathrm{rad}/\mu\mathrm{m}$. When traveling in the optical feedback loop, the beam undergoes diffraction so that the initial phase modulation is converted into an intensity modulation [15] and phase maxima gives rise to low amplitude intensity maxima on the photoconductor. In Figure 4 it is represented the profile of the grid calculated numerically in the $1D$ case, when $y = 0$ and $\varepsilon = 0.4$. In particular, in Figure 4a it is shown the profile of the grid of the light intensity on the photoconductor and in Figure 4b the corresponding θ profile. The phase grid induce a local pretilt of the liquid crystal director that can be controlled through the SPM. The local maxima of the grid act as pinning sites for the localized structures, leading to the suppression of the crosstalk. When a local pulse is sent on the photoconductor, a single localized structures is switched on and remain fixed on the grid. A three-dimensional θ profile of a single localized structures pinned on the grid is displayed in Figure 5.

The period of the spatial grid is chosen in order to match the size of the localized structures, therefore we can bring them as close one to the other as the maximum packing limit. The parameter ε ranges from 0.2 to 0.6 rad. The lower limit is dictated by the minimum modulation amplitude capable to overcome the crosstalk between localized structures, whereas the maximum limit has not to exceed the value for

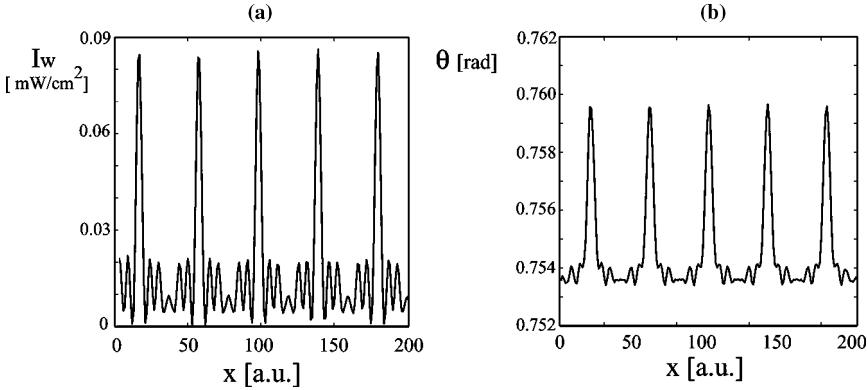

FIGURE 4 Numerical spatial profiles of: (a) the intensity on the photoconductor, (b) the tilt angle θ. The function sent on the SPM is $\varphi_{\mathrm{SPM}} = \varepsilon\cos(Kx)$.

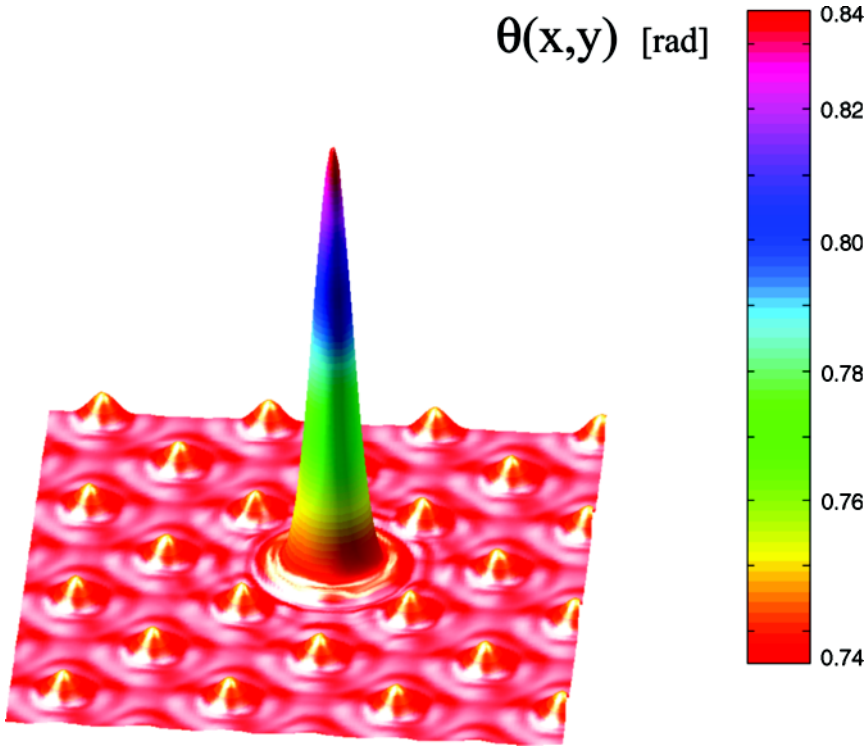

FIGURE 5 Numerical three-dimensional θ profile of a localized structures pinned on the grid.

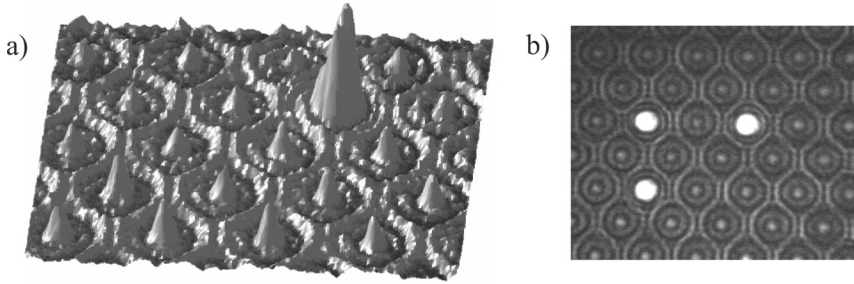

FIGURE 6 (a) Three dimensional experimental profile of the intensity on the photoconductor; (b) a configuration of three localized structures is written by flashing an image of three pulses through the SPM.

which the homogeneous stationary solution becomes unstable in favour of the pattern state. In the experiment we do not have direct access to the molecular orientation angle θ, but what we observe is the consequent localization of the light. Here, we have set $\varepsilon = 0.5$. To write localized structures either we send a sequence of local pulses or we flash an image through the SPM. We can see that once created localized structures move towards the closest local maximum of the intensity and remain attached there, as shown in Figure 6a. Indeed, the energy barrier created by the phase profile is sufficiently high to fix the localized structures at the maxima locations and to keep them stable against perturbations. By sending through the SPM an image containing the information to be stored, we can write any arbitrary configuration of localized structures. In Figure 6b are shown three localized structures stored on the LCLV.

CONCLUSIONS

In conclusion, we have shown that by introducing appropriate spatial modulation on the phase of the input beam, it is possible to control locally the reorientation angle of the liquid crystal and to suppress the crosstalk between adjacent localized structures, so that a large number of optical localized structures can be put together. Each site on the matrix can be addressed by a local pulse or by images sent through a SPM.

REFERENCES

[1] Nicolis, G. & Prigogine, I. (1977). *Self-Organization in Non Equilibrium Systems*, J. Wiley & sons: New York.
[2] For a review on pattern formation see e.g., Cross, M. & Hohenberg, P. (1993). *Rev. Modern Phys.*, *65*, 581.
[3] For a review on pattern formation in LCLV see e.g., Residori, S. (2005). *Phys. Rep.*, *416*, 201.
[4] Ramazza, P. L., Ducci, S., Boccaletti, S., & Arecchi, F. T. (2000). *J. Optics B: Quantum and Semiclassical Optics*, *2*, 399.
[5] Ramazza, P. L., Benkler, E., Bortolozzo, U., Boccaletti, S., Ducci, S., & Arecchi, F. T. (2002). *Phys. Rev. E*, *65*, 066204.
[6] Akhmanov, S. A., Vorontsov, M. A., & Ivanov, V. Yu. (1988). *JETP Lett.*, *47*, 707.
[7] Aubourg, P., Huignard, J. P., Hareng, M., & Mullen, R. A. (1982). *Appl. Opt.*, *21*, 3706.
[8] De Gennes, P. G. & Prost, J. (1993). *The Physics of Liquid Crystals* 2nd Ed., Oxford Science Publications, Clarendon Press: Oxford.
[9] Tabiryan, N. V., Sukhov, A. V., & Zel'dovich, B. Y. (1986). *Mol. Cryst. Liq. Cryst.*, *136*, 1.
[10] Khoo, I. C. (1995). *Liquid Crystals: Physical Properties and Nonlinear Optical Phenomena*, Wiley: New York.

[11] Simoni, F. (1997). *Nonlinear Optical Properties of Liquid Crystals and Polymer Dispersed Liquid Crystals*, World Scientific: Singapore.
[12] Clerc, M. G., Petrossian, A., & Residori, S. (2005). *Phys. Rev. E*, *71*, 015205.
[13] Bortolozzo, U., Residori, S., Petrossian, A., & Huignard, J. P. (2005). submitted to *Opt. Comm.* (in press)
[14] Ciaramella, E., Tamburrini, M., & Santamato, E. (1993). *Appl. Phys. Lett.*, *63*, 1604.
[15] D'Alessandro, G. & Firth, W. J. (1991). *Phys. Rev. Lett.*, *66*, 2597.
[16] Yeh, P. & Gu, C. (1999). *Optics of Liquid Crystal Displays*, Wiley: New York, 130.
[17] Firth, W. J. & Scroggie, A. J. (1996). *Phys. Rev. Lett.*, *76*, 1623.
[18] Bortolozzo, U., Ramazza, P. L., & Boccaletti CHAOS, S. (2005). *15*, 013501.
[19] Bortolozzo, U. & Residori, S. (2005). submitted to *Phys. Rev. Lett.* (in press)